Modeling of *n*-Hexadecane and Water Sorption in Wood

Ganna Baglayeva Gautham Krishnamoorthy Charles R. Frihart
Wayne S. Seames Jane O'Dell Evguenii I. Kozliak

Abstract

Contamination of wooden framing structures with semivolatile organic chemicals is a common occurrence from the spillage of chemicals, such as impregnation with fuel oil hydrocarbons during floods. Little information is available to understand the penetration of fuel oil hydrocarbons into wood under ambient conditions. To imitate flood and storage scenarios, the sorption of *n*-hexadecane (representing fuel oil hydrocarbons) and water by southern yellow pine was studied using gravimetric techniques at ambient temperature and pressure. The sorption curves obtained had three distinct regions, reflecting three different sorption phases. Lower sorption coefficients were obtained for nonpolar *n*-hexadecane than for water, leading to *n*-hexadecane maximum mass uptake values being half those of water. Lower penetration values were obtained for epoxy-coated wood compared with uncoated wood, apparently because of the inaccessibility of diffusion paths along the wood lateral surface and slower air removal from tracheids. Two models were introduced to fit the observed sorption curves into a single algebraic equation, a diffusion (Fickian) model and an empirical (non-Fickian) equation. Effective diffusion coefficients were determined under the Fickian model, resulting in ca. 10^{-7} m^2/s, 10^{-8} m^2/s, and 10^{-10} to 10^{-11} m^2/s diffusion rates for sorption in Phases 1, 2, and 3, respectively. The proposed non-Fickian model was based on first-order kinetic constants for the second sorption phase and fit the experimental data throughout all three phases. The two models were shown to corroborate each other by demonstrating that the effective surface areas of wood blocks calculated using both models' parameters were consistent with the corresponding expected physical values.

Contamination of wooden framing structures with semivolatile organic chemicals is common as a result of the spillage of chemicals (e.g., fuel oil hydrocarbons during catastrophic floods like those in Grand Forks, North Dakota, in 1997 and the U.S. Gulf coast in 2005). The ability to monitor and predict the behavior of contaminants within these wooden members can assist in environmental remediation and in the design of purposeful additive systems. The importance to more fully understand sorption of both polar and nonpolar liquids, here exemplified with water and hexadecane, is also evident for a number of other applications.

Wood is a porous heterogeneous nanocomposite, which makes it a strong absorbent for various compounds of different polarities (Marcovich et al. 1999). Wood's chemical structure consists of three main polymeric components: cellulose, hemicellulose, and lignin. A typical distribution is 44, 25, and 26 percent by weight, respectively, in southern yellow pine (Kultikova 1999). The chemical and structural differences among these three constituents influence how the wood matrix interacts with different penetrating liquids, such as water and semivolatile organic contaminants. The polar nature of cellulose and hemicellulose enables these wood components to form strong intramolecular and intermolecular hydrogen bonds with polar liquids. Conversely, the less hydrophilic lignin can attract lipophilic organic molecules, e.g., hydrocarbons.

The wood capillary microstructure (such as the geometry, type and dimensions of the cells) has a major influence on the absorption of liquids. The typical penetration channels in

The authors are, respectively, Graduate Student, Dept. of Chemistry (abaglayeva@gmail.com) and Ann and Norman Hoffman Associate Professor of National Defense/Energetics, Dept. of Chemical Engineering (gautham.krishnamoorthy@engr.und.edu), Univ. of North Dakota, Grand Forks; Team Leader, Wood Adhesives, Performance Enhanced Biopolymers, USDA Forest Serv., Forest Products Lab., Madison, Wisconsin (cfrihart@fs.fed.us); Chester Fritz Distinguished Professor, Dept. of Chemical Engineering, Univ. of North Dakota, Grand Forks (wayne.seames@engr.und.edu); Physical Science Technician, Performance Enhanced Biopolymers, USDA Forest Serv., Forest Products Lab., Madison, Wisconsin (janeodell@fs.fed.us); and Professor, Dept. of Chemistry, Univ. of North Dakota, Grand Forks (evguenii.kozliak@und.edu [corresponding author]). This paper was received for publication in December 2015. Article no. 15-00086.

Forest Prod. J. 66(7/8):401–412.
doi:10.13073/FPJ-D-15-00086

softwood are longitudinal tracheids, which are interconnected by pits, resin canals (characteristic for southern pines; Siau 1995), and rays (Fig. 1). Polar liquids can penetrate via connective flow through the lumina and by transmission through the cell walls, which can result in wood softening and swelling. It has been shown that diffusion coefficients in the longitudinal direction are at least two to three times higher than those in the transverse directions (Comstock 1970, Siau 1995). Also, the absorption is greater in open-ended tracheids formed at surfaces by sawing (Smith and Purslow 1960, Morgan and Purslow 1973, Marcovich et al. 1999). The main obstacles to the penetration of liquids into wood samples are the presence of air (Malkov et al. 2001), tyloses, gummy deposits, and bordered pits (Stone and Forderrenther 1956).

The spontaneous sorption of contaminants into wood is a relatively slow process. As a result, (1) external pressure is often applied to speed up sorption process or (2) experiments may not be continued to completion, i.e., wood saturation. However, to mimic a real-world scenario for wood contamination, long-term sorption performed under atmospheric pressure must be studied. To date, the majority of studies performed under ambient conditions reported on the sorption of either water (Comstock 1970, Chin et al. 1999, Koponen 1999, Kumaran 1999, Marcovich et al. 1999, Malkov et al. 2003, Khazaei 2008) or wood preservation agents dissolved in water (Stone and Forderrenther 1956, Smith and Purslow 1960, Petty 1978b, Krabbenhoft and Damkilde 2004, Barrera-García et al. 2008). On the other hand, the penetration of organic compounds into wood has mostly been studied under vacuum or external pressure to facilitate sorption (Morgan and Purslow 1973; Petty 1975, 1978a; Malkov et al. 2001).

Sorption in wood is frequently investigated by simple and versatile gravimetric techniques, which are dependent upon the absorbed chemical's physical properties. Usually, the wood samples are simply immersed into the liquids being studied (Smith and Purslow 1960; Morgan and Purslow 1973; Petty 1975, 1978a, 1978b; Chin et al. 1999; Kumaran 1999; Barrera-García et al. 2008; Khazaei 2008) or, in the case of water sorption, placed in humid environments (Koponen 1999, Marcovich et al. 1999, Baronas et al. 2001). Then sample mass changes with time are monitored. Other analytical techniques include deuterium exchange (Tsuchikawa and Siesler 2003), wettability and contact angle measurements (Moghaddam et al. 2013), and heating in different liquids (Stone and Forderrenther 1956).

To describe the kinetics of chemical penetration into wood, two kinds of models are usually applied: theoretical and empirical. Theoretical models typically correlate experimental data with physical laws and are based on two assumptions: (1) the sorption processes can be described by Fick's laws and (2) the diffusion coefficient is constant throughout the sorption process. This second

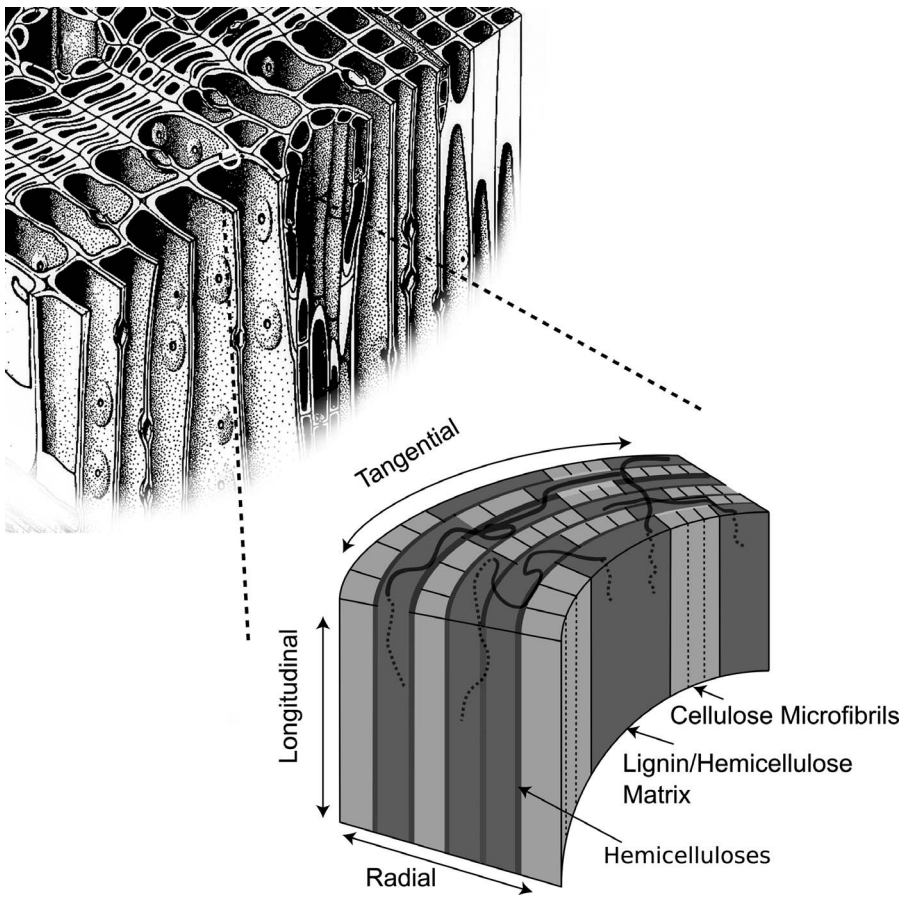

Figure 1.—Length scales and wood structure encountered by molecules undergoing mass transfer in wood. At the macroscale, fluids penetrate by bulk flow; at the nanoscale, molecules infiltrate by diffusion.

assumption is not always accurate because a number of different physical processes may occur simultaneously, particularly at the earlier stages of sorption, e.g., fast diffusion of vapors through the lumina as well as capillary rising filling the same channels.

For this reason, a single averaged diffusion coefficient is usually derived from short-term experiments using the initial linear region of the sorption curves, i.e., mass uptake versus $t^{1/2}$ (Chin et al. 1999, Kumaran 1999, Tsuchikawa and Siesler 2003, Krabbenhoft and Damkilde 2004, Khazaei 2008). This method neglects contaminant transfer into smaller capillaries and the corresponding diffusion coefficient changes that occur after reaching ca. 60 percent of the total mass uptake. By contrast, Stamm (1946) proposed calculating an effective diffusion coefficient averaged over space and time when the penetrating liquid's content reached two-thirds of the way between the initial and maximum values, i.e., 66.7 percent of total mass uptake. Another common approach is calculating the apparent diffusion coefficient at half the total sorption, i.e., 50 percent (Koponen 1999). However, such theoretical models cannot explain the slow mass uptake that is observed as the system approaches equilibrium.

Owing to the complexity of the wood matrix, different chemical–matrix interactions take place, and as a result, effective diffusion coefficients (that take into account both capillary transport and diffusion) may depend on the local chemical environment and therefore vary with both distance from the surface and sorption time. To take these changes into account and thus to describe the entire sorption process more accurately, several dual-step theoretical (Koponen 1999) and empirical (Kumaran 1999, Marcovich et al. 1999, Baronas et al. 2001, Malkov et al. 2003, Krabbenhoft and Damkilde 2004, Khazaei 2008) models have been suggested. However, none of the proposed models include both the fast initial liquid uptake at $t \approx t_0$ (a Fickian mode, where Fickian transport and capillary action dominate the mass uptake process and exhibit a dependency on the square root of time) and a molecular diffusion phase that occurs near equilibrium conditions at $t \approx t_\infty$ (a slow, potentially non-Fickian mode).

Such a slow molecular diffusion often occurs as a result of the infiltration of the cell wall. This phenomenon, called wood swelling, is well known for water and is driven by the absorption of the penetrating chemical into the polar functional groups of hemicellulose and somewhat of lignin (Frihart 2006). These hydroscopic domains expand until they are restricted by the cell-wall structure. So the wood expands outward, slightly increasing the volume in the radial and tangential directions. A similar phenomenon, although significantly less pronounced, may occur owing to the interaction of nonpolar chemicals with hydrophobic polymers, e.g., lignin.

The cases considered in the current study represent contamination of wood-based building components by both water and fuel oil hydrocarbons (represented by *n*-hexadecane) under ambient conditions that may occur during catastrophic floods. The two liquids tested, e.g., *n*-hexadecane and water, are immiscible at room temperature and are very different from each other in polarity and related physical properties. Southern yellow pine was selected for this study as a common material used in a wide range of building applications owing to its strength, durability, and cost efficiency (Kaiser 1999). The diffusion process was considered to be one-dimensional occurring along the longitudinal axis as detailed under ''Materials and Methods.''

An attempt to describe the long-term sorption process by a single equation was made. In this equation, each term refers to a specific physical process that describes particular liquid–wood matrix interactions and determines the rate limiting step of the diffusion process. The gravimetrically obtained liquid mass uptake curves were used to determine the sorption and diffusion coefficients. The extent of liquid penetration was then calculated in terms of occupied void volume. Two models were used to fit the *n*-hexadecane and water transfer kinetics into wood: a diffusion (Fickian) model and an empirical equation. Connections between the two models were then determined. The obtained results are aimed at assisting in the understanding of penetrating liquid–wood matrix interactions and long-term scenarios of contaminant penetration into wood under disastrous conditions, e.g., hurricanes and catastrophic floods, or even more benign scenarios, such as spills.

Materials and Methods

Materials and reagents

The wood used in the current study was southern yellow pine (*Pinus* spp.), with a specific gravity of 0.50 $\pm$ 0.03, which is numerically equal to density expressed in either kilograms per cubic meter or grams per cubic centimeter and a moisture fraction of 7.4 $\pm$ 0.5 percent. The specimens were taken from the lot of commercial southern yellow pine purchased by the USDA Forest Products Laboratory, Madison, Wisconsin. The wood was cut into standard sized blocks of 38 by 39 mm^2 in cross section and 150 mm in length and then kiln dried. The specimens used in this work were preselected to have no cracks, knots, or decay. All experiments were conducted between 1.2 and 1.5 years after this processing. The samples were used either as is (uncoated) or after epoxy coating. For epoxy-coated samples, all but the transverse surfaces of the wood blocks were coated with a D.E.R. 331 Liquid Epoxy Resin (Dow Chemical Co., Midland, Michigan) and a curing agent as recommended by the manufacturer. The resin was applied with a brush at least 12 hours before the experiments were initiated. This coating ensured that liquids could penetrate into the wood solely and displaced air and water could leave only via the end grain of the samples, reducing penetration from the sides (e.g., faster filling of the near-surface tracheids). To determine the physical limit (maximum percentage) of absorption, smaller (chip-size) untreated samples of 3 by 15 by 15 mm^3 were also used.

n-Hexadecane (Alfa Aesar, Ward Hill, Massachusetts) and distilled water were used as model substrates.

Experiment and data management

Three wood specimens were used for every long-term experiment described below. The resulting numerical values of sorption and/or kinetic parameters were measured separately for each specimen. Then, the mean values of three replicates were calculated for each parameter, along with the variance equal to one standard deviation and presented as such. Statistical difference between the comparable values was inferred based on the standard Student *t* test.

Equilibrium mass uptake and dry-matter content measurements

To determine the mass uptake equilibrium values for *n*-hexadecane and water sorption in uncoated and epoxy-coated wood, wood samples were fully submerged into the given liquid. For the scenarios with uncoated wood, similar experiments were repeated using chip-size wood samples. A full submersion setup with the reduced chip-size samples was used to accelerate the time needed to reach mass uptake equilibrium. The application of epoxy coating to wood chips proved to be impossible owing to their small thickness.

The samples were periodically taken out of the liquids, blotted with paper tissues, and weighed. The wood block samples were soaked for ca. 2 years in either *n*-hexadecane or water until they attained a constant mass. The wood chips reached equilibrium in 21 days.

To determine the dry-matter content (DMC) of southern yellow pine (i.e., the weight of the material after the removal of naturally present entrained water), both full-size wood samples and wood chips were oven-dried at 100°C for 7 days until their weight became constant.

Mass uptake measurements

Gravimetric measurements covering the full range to near equilibrium sorption of *n*-hexadecane and water by wood samples were performed according to the following four scenarios:

1. *n*-hexadecane diffusion in uncoated wood,
2. *n*-hexadecane diffusion in epoxy-coated wood,
3. water diffusion in uncoated wood, and
4. water diffusion in epoxy-coated wood.

Wood blocks were placed vertically in 200-mL glass beakers along with the liquid substrate (*n*-hexadecane in Scenarios 1 and 2, and water in Scenarios 3 and 4). The liquid covered ca. 10 mm in height of the wood samples. The liquid's level was maintained throughout the entire experiment by periodic refilling. The beakers were capped with aluminum foil, which was taped to the glass when the time intervals between the measurements exceeded 1 day. The experiments were performed in an air-conditioned building under the following conditions: temperature at 22°C ± 2°C, ambient pressure, and near 55 percent relative humidity. In select long-term experiments (whenever necessary), 5 mM aqueous sodium azide solution was used instead of water to prevent any mold growth.

Gravimetric kinetic measurements were conducted at suitable intervals of time based on an expected rate of absorption. At the allotted times the wood blocks were taken out, gently wiped with a lint-free tissue to remove sorbent droplets from the sample's surface, weighed, and then replaced back into the beaker. The initial reading was performed at 7 minutes, and the final reading at 210 days. At completion the difference between two consecutive mass determinations (being 10 days apart) of each of the samples was insignificant. Using this arrangement, enough data points were taken to capture the changes in sorption parameters with an increase in the amount of absorbed liquid.

Evaluation of sorption parameters

Data on the mass transfer of penetrating liquids into wood at different time periods were evaluated in terms of mass uptake (M) and degree of penetration (PD). Mass uptake was calculated as the sorption amount (i.e., the difference between wood block weights at times t and $t_0 = 0$ expressed as W_t and $W_{t=0}$, respectively) over the initial weight of wood $W_{t=0}$ (Siau 1995):

$$M = \frac{W_t - W_{t=0}}{W_{t=0}} \tag{1}$$

The degree of penetration was defined as the fraction of the theoretical maximum void space in the wood blocks (V_{voids}) filled with liquids (i.e., the absorbed liquid [$V_{\text{absorbed liquid}}$] and initially present water [$V_{\text{inside water}}$]; Malkov et al. 2001):

$$\text{PD} = \frac{V_{\text{inside water}} + V_{\text{absorbed liquid}}}{V_{\text{voids}}} \tag{2}$$

The volume of absorbed liquid was calculated by subtracting the initial weight of the ambient wood from the weight of wood blocks at any given time, t:

$$V_{\text{absorbed liquid}} = \frac{W_t - W_{\text{wet wood}}}{\rho_{\text{absorbed liquid}}} \tag{3}$$

where $\rho_{\text{absorbed liquid}}$ is the density of absorbed liquid (i.e., *n*-hexadecane or water).

The volume of water initially present in the wood sample ($V_{\text{inside water}}$) and the maximum available void space (V_{voids}) were calculated using DMC, which was determined experimentally as follows (Malkov et al. 2001):

$$\text{DMC} = \frac{W_{\text{dry wood}}}{W_{\text{ambient wood}}} \tag{4}$$

where $W_{\text{ambient wood}}$ and $W_{\text{dry wood}}$ are the ambient and ovendried wood sample weights, respectively. Thus (Stone and Forderrenther 1956, Malkov et al. 2001),

$$V_{\text{inside water}} = \frac{W_{\text{ambient wood}} - W_{\text{dry wood}}}{\rho_{\text{water}}} = \frac{W_{\text{ambient wood}} \cdot (1 - \text{DMC})}{\rho_{\text{water}}} \tag{5}$$

$$V_{\text{voids}} = V_{\text{dry wood}} - V_{\text{wood substance}} \tag{6}$$

where ρ_{water} is the density of water at 20°C, $V_{\text{dry wood}}$ and $V_{\text{wood substance}}$ are the volumes of ovendried wood and wood's physical material excluding its void volume, respectively:

$$V_{\text{dry wood}} = \frac{W_{\text{dry wood}}}{\rho_{\text{dry wood}}} = \frac{W_{\text{ambient wood}} \cdot \text{DMC}}{\rho_{\text{dry wood}}} \tag{7}$$

$$V_{\text{wood substance}} = \frac{W_{\text{dry wood}}}{\rho_{\text{wood substance}}} = \frac{W_{\text{ambient wood}} \cdot \text{DMC}}{\rho_{\text{wood substance}}} \tag{8}$$

where $\rho_{\text{dry wood}}$ and $\rho_{\text{wood substance}}$ are the densities of ovendried wood and of the wood's physical material excluding its void volume, respectively. $\rho_{\text{wood substance}}$ was assumed to be 1.5 kg/m^3 (Stamm 1964) for all wood samples used and to be constant throughout the experiments. The wood volume remained virtually unchanged upon drying. Wood volume slightly increased (by less than 5%) in long-term experiments with water owing to wood swelling. However, given its small magnitude, the resulting volume

was approximated as the original volume of wood blocks. The sorption curves were presented as $M = f(t^{1/2})$.

The sorption coefficient of the penetrating liquids, *n*-hexadecane and water, in wood (S, kg/m^2 s$^{1/2}$) was estimated as the slope of

$$\frac{(W_t - W_{t=0})}{A} = f(t^{1/2}) \tag{9}$$

where A is the surface area of the wood block in square meters exposed to the penetrating liquid:

$$A = (hw + 2dh + 2dw) \tag{10}$$

where h and w are the height and the width of a wood block (hw defining the block base), and d is the depth at which the wood block was immersed in the liquid (i.e., 10 mm), measured in radial, tangential, and longitudinal directions, respectively. Thus, the parameter S used in this study is similar to the earlier used ''water sorption coefficient'' (Kumaran 1999) applied to both water and *n*-hexadecane. For wood samples with epoxy-sealed sides, the same value of A was used to exclude the influence of this arbitrary parameter. Given the prevalence of end-grain sorption, the bulk of the liquid's flux penetrates just through the wood sample base. Yet, Equation 10 was used to assure consistency with previously reported values (Kumaran 1999). The same approach was used for calculating diffusion coefficients as described in the next section. The issue of effective sorption area is addressed in the final section of this article.

Fickian model: Determination of diffusion coefficients

Un–steady state one-dimensional diffusion can be described by Fick's second law as

$$\frac{\partial C}{\partial t} = -D\frac{\partial^2 C}{\partial x^2} \tag{11}$$

The initial region of a liquid's sorption curve is typically believed to follow Fickian behavior if Equation 11 is valid to at least 60 percent of the total mass uptake, regardless of the material thickness (Chin et al. 1999). For one-dimensional diffusion through a planar sheet of length L subject to the boundary conditions:

$$\begin{aligned} &\text{at } x = 0,\ C = C_1,\ t \geq 0,\\ &\text{at } x = L,\ C = 0,\ t \geq 0, \text{ and}\\ &\quad C = C_0 \text{ for } 0 \leq x \geq L \text{ at } t = 0 \end{aligned}$$

i.e., the entire sheet is initially at a uniform concentration of C_0 throughout at time $t = 0$. If W_t denotes the total amount of diffusing substance that has entered the domain at time t and W_∞ is the corresponding quantity after infinite time, then the solution of Equation 11 was presented for application by Siau (1995) and documented as equation 4.23 in Crank (1975, p. 50) as follows:

$$\left(\frac{W_t - W_0}{W_\infty - W_0}\right) = \left(1 - \frac{8}{\pi^2}\sum_{n=0}^{\infty}\frac{1}{(2n+1)^2}e^{-D(2n+1)^2\pi^2 t/L^2}\right) \tag{12}$$

For short time periods, Equation 12 can be further simplified to Equation 13, again presented by Siau (1995) and documented as equation 4.20 in Crank (1975, p. 48):

$$\frac{W_t - W_{t=0}}{W_{t=\infty} - W_{t=0}} = \left(\frac{2}{L\sqrt{\pi}}\right)\sqrt{Dt} \tag{13}$$

where L is the distance through a planar sheet and D is the effective diffusion coefficient with only the real part of the infinite series solution taken into consideration. It is of note that conventional ''short'' time periods for Equation 13 refer to relatively small values of the product, Dt, rather than just t per se. Thus this approximation is valid for both the initial sorption phase (short times, fast diffusion) and final phase (long times but very slow diffusion).

Assuming diffusion only in the longitudinal direction, the solution to the one-dimensional diffusion equation, Equation 13, can be extended to rectangular-shaped wood blocks (Kumaran 1999):

$$\frac{W_t - W_{t=0}}{W_{t=\infty} - W_{t=0}} = \frac{2}{\sqrt{\pi}}\left(\frac{A}{V}\right)\sqrt{Dt} \tag{14}$$

where A is the surface area of a wood block in contact with the liquid (determined by Eq. 10) and V is the volume of a wood block:

$$V = hwL \tag{15}$$

where h, w, and L are the block dimensions defined above. The alternative value $A = V/L = hw$ instead of that shown in Equation 10, i.e., just a base of the wood blocks used, would be more suitable in terms of usage of Equation 13. However, the use of this value would be inconsistent with that used for sorption coefficient measurements (Kumaran 1999) as well as earlier reported values of D (Siau 1995). For $A = hw$, all of the values of effective diffusion coefficients reported in this work have to be multiplied by the factor of $[(hw + 2dw + 2dh)/hw]^2 = [(7.6 + 7.8 + 3.9 \times 3.8)/3.9 \times 3.8]^2 = 4.15$.

Equation 14 was derived for single-phase sorption processes where the diffusion rate is constant throughout the time of the experiment. However, in the systems studied, three different regions were observed in the sorption curves, thus corresponding to three distinct diffusion mechanisms as discussed in detail under ''Results and Discussion.'' Hence, modifications to Equation 14 are required. The simplest way to represent a multiphase process is by assuming that there are several independent *n*-hexadecane–water fluxes, each with a different diffusion rate and therefore a different diffusion coefficient (Eqs. 16 to 18):

$$\frac{\partial C}{\partial t} = -D_1\frac{\partial^2 C}{\partial x^2} \tag{16}$$

$$\frac{\partial C}{\partial t} = -D_2\frac{\partial^2 C}{\partial x^2} \tag{17}$$

$$\frac{\partial C}{\partial t} = -D_3\frac{\partial^2 C}{\partial x^2} \tag{18}$$

Each of these equations can be solved similarly to Equation 14 as follows:

$$\frac{W_{t1} - W_{t=0,1}}{W_{t=\infty,1} - W_{t=0,1}} = \frac{2}{\sqrt{\pi}}\left(\frac{A}{V}\right)\sqrt{D_1 t} \tag{19}$$

$$\frac{W_{t2} - W_{t=0,2}}{W_{t=\infty,2} - W_{t=0,2}} = \frac{2}{\sqrt{\pi}}\left(\frac{A}{V}\right)\sqrt{D_2 t} \tag{20}$$

$$\frac{W_{t3} - W_{t=0,3}}{W_{t=\infty,3} - W_{t=0,3}} = \frac{2}{\sqrt{\pi}}\left(\frac{A}{V}\right)\sqrt{D_3 t} \tag{21}$$

where W_{t1}, W_{t2}, and W_{t3} are the weights of samples in sorption Phases 1, 2, and 3, respectively, at any time t; $W_{t=0,1}$, $W_{t=0,2}$, and $W_{t=0,3}$ are the weights of each sample at time $t = 0$; and $W_{t=\infty,1}$, $W_{t=\infty,2}$, and $W_{t=\infty,3}$ are the weights of the samples at equilibrium. Then, the mass balance is closed as follows:

$$M_t = M_{t1} + M_{t2} + M_{t3} \tag{22}$$

$$M_{t=0} = M_{t=0,1} + M_{t=0,2} + M_{t=0,3} \tag{23}$$

$$M_{t=\infty} = M_{t=\infty,1} + M_{t=\infty,2} + M_{t=\infty,3} \tag{24}$$

where M_0, M_t, and M_∞ represent the total amounts of liquid diffused at $t_0 = 0$, any time t, and $t = \infty$, respectively. The final expression for the model with three diffusion fronts will then be

$$\frac{W_t - W_{t=0}}{W_\infty - W_{t=0}} = \frac{W_{t1} - W_{t=0,1}}{W_\infty - W_{t=0}} + \frac{W_{t2} - W_{t=0,2}}{W_\infty - W_{t=0}} + \frac{W_{t3} - W_{t=0,3}}{W_\infty - W_{t=0}}$$

or

$$W_t - W_{t=0} = (W_{t1} - W_{t=0,1}) + (W_{t2} - W_{t=0,2}) + (W_{t3} - W_{t=0,3}) \tag{25}$$

and the Fickian model of a three-phase sorption process can be described as

$$W_t - W_{t=0} = \begin{cases} \dfrac{2}{\sqrt{\pi}}\left(\dfrac{A}{V}\right)\sqrt{D_1 t}(W_{t=\infty,1} - W_{t=0,1}) & \text{when } t \le t_{\infty,1} \\ \dfrac{2}{\sqrt{\pi}}\left(\dfrac{A}{V}\right)\sqrt{D_2 t}(W_{t=\infty,2} - W_{t=0,2}) + (W_{t=\infty,1} - W_{t=0}) & \text{when } t_{\infty,1} < t \le t_{\infty,2} \\ \dfrac{2}{\sqrt{\pi}}\left(\dfrac{A}{V}\right)\sqrt{D_3 t}(W_{t=\infty,3} - W_{t=0,3}) + (W_{t=\infty,2} - W_{t=0}) & \text{when } t > t_{\infty,2} \end{cases} \tag{26}$$

where D_1, D_2, and D_3 are effective diffusion coefficients for sorption Phases 1, 2, and 3, respectively, determined using Equations 19 to 21.

The resulting Fickian model defined by Equation 26 was used to describe the long-term (i.e., 210 days) sorption process of *n*-hexadecane and water in wood by applying Fick's laws.

Empirical modeling of the sorption process

An empirical description of *n*-hexadecane and water sorption in uncoated or epoxy-coated wood was developed based on the model formulated by Khazaei (2008) for water sorption. Two sorption phases were distinguished and described by

$$M = \left(\frac{W_t - W_{t=0}}{W_{t=0}}\right) = M_{\text{ret}}(1 - e^{-t/T_{\text{ret}}}) + k_{\text{rel}} t \tag{27}$$

where rel is the relaxation phase; ret is the retardation phase; T_{ret} is the time required to reach 63 percent of the total retarded moisture content, M_{ret}; and k_{rel} is the rate of absorption in the relaxation phase in 1/time when the mass uptake, M, is measured as a fraction (%/time if M reflects the percentage).

In the current study, this model (Eq. 27) was further developed by separating Phase 1 from the retardation phase (Fig. 2). Hence, the sorption process was described by the following equation:

$$M = \left(\frac{W_t - W_{t=0}}{W_{t=0}}\right) = \begin{cases} k_1\sqrt{t} + M_{\text{initial}} & \text{when } M \le M^* \\ M_{\text{ret}}(1 - e^{-k_2 t}) + k_3 t & \text{when } M > M^* \end{cases} \tag{28}$$

where k_1, k_2, and k_3 are the sorption rate constants for the first, second, and third mass uptake periods (i.e., sorption Phases 1, 2, and 3), respectively, and M_{initial}, M^*, and M_{ret} are the mass uptake values indicating the beginning of sorption Phases 1, 2, and 3, respectively. While the wood sample was completely immersed into the liquid in the original work of Khazaei, only partial immersion was used in this study, as described above.

The values of k_1 and M_{initial} were calculated as the slope and y intercept of a straight line based on the first part of the experimentally obtained sorption curve. The values of k_3 and M_{ret} were estimated by extrapolation from the last part of the sorption curve, as its slope and y intercept, respectively. The value k_2 corresponds to the time at 63 percent of M_{ret} where $0.63 = 1 - e^{-k_2 t}$, i.e., $k_2 = t^{-1}$. All of these parameters can be determined graphically, as shown in Figure 2.

M^* was determined empirically by calculating mass uptake values for the entire sorption process using only the second part of Equation 28, i.e., when $M > M^*$. M^* represents the point (corresponding to t^*; Fig. 2), after which the experimental data no longer fit a square-root

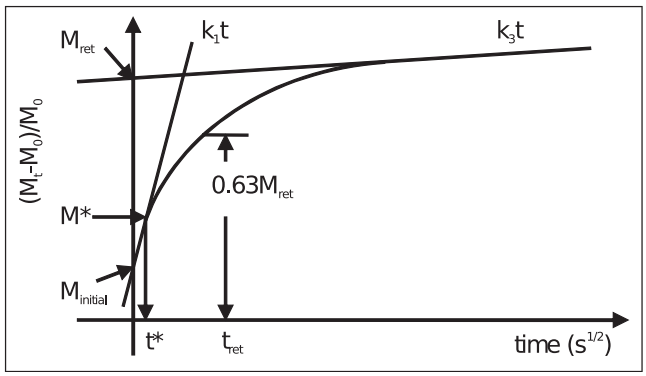

Figure 2.—A graphical representation of the empirical sorption model expressed by Equation 28. The parameters shown are explained in the text below Equation 28; their determined values are listed in Table 3.

model and result in calculated mass uptake values lower than the actual experimental values.

The experimental values of D_i are valid only for certain times when they were measured. With time, a slow increase of D_2, and particularly D_1, was observed. Perhaps this is owing to gradual wood drying resulting in widening of capillaries transporting the penetrating liquids.

To validate the proposed empirical model, the model's ability to fit the experimental data obtained for the sorption of *n*-hexadecane and water in uncoated and epoxy-coated wood was measured using the Pearson correlation coefficient (R^2) and the root mean square error (RMSE).

Connection of two models through an empirical parameter

To connect the Fickian and empirical models, the effective surface areas of wood samples subject to *n*-hexadecane and water sorption were calculated as

$$A_{\text{eff}} = \frac{D_i}{k_i} \tag{29}$$

where D_i is the effective diffusion coefficients for sorption Phases 1, 2, or 3 as determined by Equation 26, and k_i is the sorption rate constants for sorption Phases 1, 2, or 3 as calculated by Equation 28. The way they are defined, these empirical parameters are merely conversion factors having dimensions of squared length. They may or may not reflect the actual dimensions or parameters (i.e., lumen area) of the wood samples used.

Results and Discussion

Equilibrium sorption parameters

Table 1 shows the maximum penetration degree, PD (Eq. 2, determined for $t = t_{730\ \text{days}}$) and the equilibrium mass uptake (Eq. 1 for $t = t_{730\ \text{days}}$) for water and *n*-hexadecane diffusing into uncoated and epoxy-coated wood samples. Slightly smaller values of maximum *n*-hexadecane sorption were obtained for uncoated wood blocks than for uncoated wood chips, probably because of incomplete removal of air from the tracheids and as a result of incomplete saturation in the wood blocks. In contrast to the results for *n*-hexadecane, a nonpolar slow-absorbing hydrocarbon, the maximum uptake values for water were statistically indistinguishable between uncoated wood blocks and uncoated wood chips. Because water is a polar chemical, it appears to form strong hydrogen bonds with the polar components of wood (i.e., cellulose and hemicellulose). This appears to facilitate air displacement within pits, and thus, the contaminant may reach its equilibrium mass uptake quicker. A similar experiment with epoxy-coated wood chips was not conducted owing to the small size and irregularity of the samples (chips) used in these maximum uptake experiments, prohibiting a consistent application of epoxy coating.

Overall, the values for the maximum sorption in uncoated and epoxy-coated wood for water were about twice those for *n*-hexadecane (Table 1). This may be owing to differences in the two penetrating liquids' physical properties and the resulting different liquid–matrix interactions. In terms of kinetics, water is less viscous in comparison with *n*-hexadecane and thus may fill all wood voids, even those that are hard to access, e.g., by pushing out entrained air and diffusing through pits. The high polarity of water improves its interactions with polar cellulosic walls, thus enabling a higher thermodynamic sorption capacity. In addition, water is a well-known wood-swelling reagent and thus may transport through the cell walls themselves. *n*-Hexadecane, as a nonpolar chemical of relatively large molecular size, most likely diffuses only through large easily accessible tracheids, leaving the remaining voids filled with air. As a result, the maximum penetration degree (i.e., percentage of filled wood voids) for *n*-hexadecane was ca. 52 percent, whereas water filled 100 percent of the available wood voids (Table 1).

The maximum PD and maximum sorption values for *n*-hexadecane and water in uncoated and epoxy-coated wood blocks (Table 1) were further used to monitor the progress of the sorption process in all subsequent experiments (see results below). The next two sections will introduce the experimentally observed sorption phases and then the quasi-equilibrium values of PD obtained after the end of particular sorption phases.

Sorption phases

Mass uptake of *n*-hexadecane and water into both uncoated and epoxy-coated wood was found to be proportional to the square root of the immersion time, with three distinct phases being clearly discernible, to be denoted henceforth as sorption Phases 1 to 3, respectively (Fig. 3). For all investigated scenarios, the isotherms obtained were convex to the x axis (i.e., the square root of time in second$^{1/2}$; Fig. 3), indicating the rapid initial uptake of liquid (Phase 1), apparently because of pore filling on the surface, multilayered absorption, and (in the case of water) wood swelling. The large slope (i.e., sorption rate, S) observed initially for Phase 1 starts to decline after the first hour of sorption,

Table 1.—Maximum penetration degree and equilibrium mass uptake for the one-dimensional sorption of water or n*-hexadecane through uncoated and epoxy-coated wood blocks and uncoated wood chips.*[a]

			Maximum penetration degree, PD_∞ (%)[b]	Equilibrium mass uptake, M_∞ (%)[c]	
Scenario	Penetrating liquid	Matrix	Wood blocks (150 × 38 × 39 mm^3)	Wood blocks (150 × 38 × 39 mm^3)	Wood chips (3 × 15 × 15 mm^3)
1	*n*-Hexadecane	Uncoated wood	51.2 ± 0.7	69.9 ± 3.9	85.1 ± 1.3
2		Epoxy-coated wood	51.8 ± 2.6	59.1 ± 2.4	NA[d]
3	Water	Uncoated wood	107.5 ± 2.6	166.7 ± 18.2	175.1 ± 27.7
4		Epoxy-coated wood	120 ± 28	137.2 ± 21.9	NA

[a] The results are presented as mean values of three replicates ± one standard deviation.

[b] Maximum penetration degree values were calculated using Equation 2, $t = t_{730\ \text{days}}$.

[c] Equilibrium mass uptake values were calculated using Equation 1, $t = t_{730\ \text{days}}$ for wood blocks and $t = t_{21\ \text{days}}$ for wood chips.

[d] NA = not applicable owing to the small size and irregularity of the samples, prohibiting a consistent application of epoxy coating.

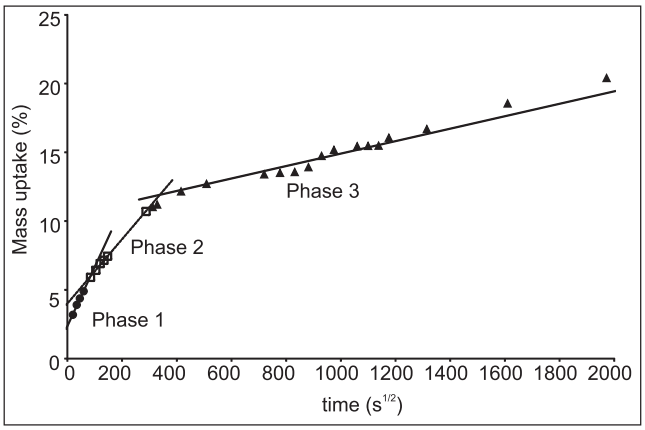

Figure 3.—Mass uptake of n*-hexadecane into uncoated wood as a function of the square root of the immersion time. Phases 1 to 3 correspond to three observed sorption phases described in the text.*

signifying the beginning of Phase 2. During the third and final phase, an extremely slow sorption was observed. This final phase continues until the full saturation of the sample is reached. Typically, only two sorption phases are reported in the literature, with Phases 1 and 2 combined followed by a long transition to Phase 3 (Smith and Purslow 1960, Morgan and Purslow 1973). The clear presence of three phases has not previously been reported except for one recent study (Moghaddam et al. 2013). However, the first two sorption phases in that study occurred within the first 180 seconds of the experiment, i.e., before Phase 1 considered in this work.

Table 2 summarizes the endpoint values of the mass uptake and sorption coefficients for the three phases of *n*-hexadecane and water sorption in uncoated and epoxy-coated wood. Phases 1 and 2 lasted 6 and 48 hours for water and *n*-hexadecane in uncoated wood (t_2 in Table 2), respectively, whereas Phase 3 took ca. 210 days (t_3 in Table 2) for both penetrating liquids. The effects of (1) the polarity of the penetrating liquid and (2) covering the wood samples' lateral sides with epoxy are considered separately for all three observed sorption phases below.

Phase 1 appears to be caused by unhindered liquid absorption (perhaps combined with faster air displacement), when readily accessible open-ended tracheids, which are made by sawing on the rough end grain surface, are filled quickly. Greater sorption coefficients and thus mass uptake for water in comparison with *n*-hexadecane (S_1 and M_1, respectively, Phase 1; Table 2) can be attributed to water's affinity to the mostly polar–hygroscopic matrix of wood tracheids, although a higher vapor pressure of water may also be a factor. When the lateral pores were covered with epoxy, the sorption coefficient for water decreased by a factor of two, whereas for nonswelling *n*-hexadecane it was similar in both uncoated and epoxy-coated wood (S_1, Phase 1; Table 2). Apparently, coating the lateral pores increases resistance to air displacement. It is well known that lateral transport is hindered in epoxy-coated wood making air displacement more difficult and resulting in lower sorption rates (Malkov et al. 2001). This factor appears to become the limiting factor for water sorption but not for the slower moving *n*-hexadecane. Besides gradual air displacement, this hydrocarbon may simply dissolve small air bubbles owing to its affinity to nonpolar molecules of gases in the entrained air.

During Phase 2, relatively large tracheids interconnected by smaller diameter pits near the surface appear to be filled with the sorbing liquid. At the end of this step, when all of the lateral voids are filled (cf. Fig. 1), the mass uptake values for water and *n*-hexadecane were similar, with smaller values obtained for the epoxy-covered wood samples (M_2, Phase 2; Table 2). Unlike Phase 1, the endpoint mass uptake values for Phase 2 were lower in epoxy-covered wood for both water and *n*-hexadecane (S_2, Phase 2; Table 2). This effect may also be explained by air bubble resistance. With only smaller amounts of diffusing *n*-hexadecane, there may no longer be sufficient liquid to dissolve entrained air bubbles, thus eliminating the difference with water. As the fraction of filled voids increases, the effective sorption rate necessarily slows down as the difficulty to fill voids becomes the dominant factor, thus ultimately leading to the third, final diffusion phase. The quantitative differences between all four scenarios, water and *n*-hexadecane with and without the epoxy, are considered in the following sections, along with the values of diffusion coefficients.

Phase 3, an extremely slow final step of sorption, can be attributed to molecular diffusion, the process by which a fluid migrates and spreads itself through capillaries and, in the case of polar water, the cellular walls of the wood. Because most of the air has already been displaced (Smith and Purslow 1960) and all the surface voids filled during Phases 1 and 2, liquid movement is restricted to the bulk of the wood matrix only, resulting in similar sorption rates and uptake values in uncoated versus epoxy-coated wood for both *n*-hexadecane and water (S_3, Phase 3; Table 2). For the same reason, wood swelling becomes the most important factor, resulting in a 10 times higher sorption rate for water than for *n*-hexadecane.

The experiments were halted after 210 days when the amount of water in the epoxy-coated samples reached its equilibrium mass uptake value (M_3, Phase 3, Table 2 vs. M_∞, Table 1). A slightly greater endpoint value of water mass uptake in coated wood was presumably a result of more cracks caused by wood swelling. Achieving complete wood saturation with *n*-hexadecane was projected to take another year or two but would not increase the accuracy of Phase 3 models because the sorption rate is essentially constant at 210 days.

The endpoint values of M_1 and M_2 from Table 2 were used to calculate effective diffusion coefficients for Phases 1 and 2, respectively, using Equation 26 (i.e., when $t \leq t_{\infty,1}$ and $t_{\infty,1} < t \leq t_{\infty,2}$, respectively). To estimate effective diffusion coefficients for Phase 3, the equilibrium mass uptake values obtained for smaller size wood chips (M_∞; Table 1) were applied using Equation 26 (i.e., when $t > t_{\infty,2}$).

Quasi-equilibrium uptake values at the end of Phases 1 and 2

During Phases 1 and 2, when liquids penetrate mostly into large and open-ended tracheids, the PD's for *n*-hexadecane and water were found to be similar (PD_1 and PD_2, Phases 1 and 2, respectively; Table 2). However, lower PD values were obtained for epoxy-coated wood samples than for uncoated wood samples. This effect is probably due to the inaccessibility of diffusion paths along the wood's lateral

Table 2.—The endpoint values of penetration degree and mass uptake plus their corresponding sorption and diffusion coefficients (Fickian model) for different phases of the one-dimensional sorption of water or n*-hexadecane through uncoated and epoxy-coated wood blocks.*[a]

			Sorption Phase 1				
Scenario	Penetrating liquid	Matrix	Time, t_1 (h)	Penetration degree, PD_1 (%)[b]	Mass uptake, M_1 (%)[c]	Sorption coefficient, S_1 ($\times 10^{-3}$ kg/m^2 s$^{1/2}$)[d]	Effective diffusion coefficient, D_1 ($\times 10^{-7}$ m^2/s)[e]
1	*n*-Hexadecane	Uncoated wood	1	12.6 ± 2.9	4.6 ± 0.4	13.4 ± 0.0	7.2 ± 1.7
2		Epoxy-coated wood	1	9.9 ± 1.3	4.9 ± 0.8	13.5 ± 0.0	7.4 ± 0.1
3	Water	Uncoated wood	1	13.8 ± 2.0	7.1 ± 0.5	29.9 ± 0.9	5.9 ± 0.9
4		Epoxy-coated wood	1	10.4 ± 1.9	5.2 ± 0.7	19.7 ± 0.0	6.7 ± 0.1
			Sorption Phase 2				
Scenario	Penetrating liquid	Matrix	Time, t_2 (h)	Penetration degree, PD_2 (%)	Mass uptake, M_2 (%)	Sorption coefficient, S_2 ($\times 10^{-3}$ kg/m^2 s$^{1/2}$)	Effective diffusion coefficient, D_2 ($\times 10^{-8}$ m^2/s)
1	*n*-Hexadecane	Uncoated wood	48	23.8 ± 3.2	13.5 ± 1.2	6.9 ± 0.6	0.9 ± 0.3
2		Epoxy-coated wood	31	14.2 ± 2.1	9.3 ± 1.0	3.4 ± 0.4	1.2 ± 0.4
3	Water	Uncoated wood	6	19.7 ± 2.3	13.1 ± 1.4	18.4 ± 1.8	7.6 ± 0.1
4		Epoxy-coated wood	5	13.1 ± 2.3	8.4 ± 0.8	9.4 ± 1.1	8.4 ± 0.3
			Sorption Phase 3				
Scenario	Penetrating liquid	Matrix	Time, t_3 (h)	Penetration degree, PD_3 (%)	Mass uptake, M_3 (%)	Sorption coefficient, S_3 ($\times 10^{-3}$ kg/m^2 s$^{1/2}$)	Effective diffusion coefficient, D_3 ($\times 10^{-11}$ m^2/s)
1	*n*-Hexadecane	Uncoated wood	5,040	50.0 ± 3.4	34.6 ± 5.3	1.5 ± 0.1	3.2 ± 1.3
2		Epoxy-coated wood	5,040	44.6 ± 2.1	41.0 ± 6.9	1.1 ± 0.1	4.9 ± 2.1
3	Water	Uncoated wood	5,040	100.4 ± 6.5	95.7 ± 13.2	10.0 ± 2.5	20.2 ± 9.5
4		Epoxy-coated wood	5,040	123.6 ± 8.7	139.1 ± 23.9	9.2 ± 0.2	20.1 ± 6.2

[a] The results are presented as mean values of three replicates ± one standard deviation.
[b] Penetration degree values were calculated by using Equation 2.
[c] Mass uptake values were calculated by using Equation 1.
[d] Sorption coefficients were estimated as a slope of $(W_t - W_\infty)/A = f(t^{1/2})$.
[e] Effective diffusion coefficients were calculated using Equation 26.

surface. During Phase 3, once the lateral superficial layers and large tracheids of wood are filled, further penetration of liquids takes place via the bordered small-diameter pits and is therefore restricted by the size and polarity of the penetrating liquid. As a result, the PD for polar water was found to be twice that of *n*-hexadecane (PD_3, Phase 3; Table 2). The observed result of greater than 100 percent wood pore filling with water in epoxy-coated wood samples can be explained by space-restricted wood swelling, which results in water accumulation in wood cell walls.

Effective diffusion coefficients: The Fickian sorption model

The equilibrium and quasi-equilibrium solvent uptake values have been considered in the previous sections, along with the qualitative trends in sorption rates. Their accurate estimation was essential for calculating the effective diffusion rates, which are addressed quantitatively throughout the rest of the study. Phase 1 effective diffusion coefficients of *n*-hexadecane and water in either uncoated or coated wood were found to be similar despite large differences in molecular size and polarity between these two liquids (D_1, Phase 1; Table 2). This observation confirms the hypothesis of initial filling of readily accessible near-surface voids owing to simple sorption.

By contrast, in Phase 2 the effective diffusion coefficient for water was approximately one order of magnitude greater than that for *n*-hexadecane (D_2, Phase 2; Table 2). Apparently, capillary rising becomes the predominant process during Phase 2, and thus the absorbing liquid's physical properties and its interactions with the wood matrix influence the sorption speed. However, at this point the sorption process is not completely finished, because a rapid significant increase of mass uptake values is observed (M_1, Phase 1 vs. M_2, Phase 2; Table 2).

Coating the wood samples with an epoxy resin did not alter this qualitative trend. The numerical values of Phase 2 effective diffusion coefficients were statistically the same for the coated and uncoated wood (D_2, Phase 2; Table 2). This similarity in specific (mass-independent) D_1 and D_2 values contrasts with the observed significant changes in the corresponding bulk (i.e., involving the actual absorbed mass) values of sorption coefficients for coated and noncoated wood samples (Table 2). While the bulk values of S are smaller for coated samples as a result of physical obstacles, these obstacles do not pertain to the movement of the liquid's front, which is used to calculate the value of the effective diffusion coefficients. Diffusion in coated samples may actually be slightly faster than reflected in Table 2 given the lack of a lateral flux in epoxy-coated samples. This flux would reduce the effective values of sorption area (parameter A in Eq. 26) in coated wood with the corresponding increase of D_1 and D_2. However, given the significant prevalence of end-grain sorption compared with lateral, this effect should be deemed insignificant.

Once the two fast sorption phases were over, both penetrating liquids exhibited much smaller Phase 3 effective diffusion coefficients of ca. 10^{-10} to 10^{-11} m^2/s (D_3, Phase 3; Table 2). These numerical values are commensurate with molecular diffusion. Phase 3 diffusion coefficients of water (D_3) were larger than those of *n*-hexadecane, as expected,

because water is a wood-swelling liquid, and this swelling facilitates molecular diffusion.

The calculated effective diffusion coefficients for sorption Phases 1 to 3 (Table 2) were used to calculate the theoretical mass uptake values of *n*-hexadecane and water in uncoated and epoxy-coated wood and to construct theoretical Fickian model sorption curves (i.e., $M = f(t^{1/2})$), as shown in Figure 4. The experimental sorption profiles were then matched to these Fickian model predictions (Fig. 4).

Based on the results reported here, the Fickian model is efficient not only in describing the experimental behavior of *n*-hexadecane and water within a wide time range (Fig. 4) but also in predicting effective diffusion coefficients for all three sorption phases (*D*; Table 2), which to the best of our knowledge, has not previously been reported. These results lead to a better understanding of penetrating liquid–wood matrix interactions and diffusion processes in wood samples, e.g., the difference between absorption of polar and nonpolar chemicals.

An empirical model of the multistep sorption process

The effective diffusion coefficients of *n*-hexadecane and water in wood (*D*; Table 2) were obtained under the hypothesis that these heterogeneous sorption processes follow Fick's second law. However, the sorption curve displays an abrupt change of its slope at least twice during the process (Fig. 3), suggesting a change of rate limiting mechanism at each inflection. The Fickian model cannot predict the time at which this change would occur. This time can only be found using an empirical model, i.e., the description of the sorption behavior of *n*-hexadecane and water in wood as a non-Fickian process (Eq. 28). The rationale for using this model is that it describes a similar process (fast initial absorption, which then slows down significantly) using simple combinations of linear terms and first-order kinetic constants, which are presented as their reciprocal values called relaxation times (Eq. 27). The estimated non-Fickian model parameters and goodness of fit between theoretical and experimental data are summarized in Table 3.

The model, graphically represented in Figure 2, was developed based on a model suggested by Khazaei (2008; Eq. 27). Originally, only two sorption phases of liquid (water, in particular) uptake in wood samples were described (Khazaei 2008), neglecting the initial rapid mass uptake, i.e., Phase 1.

Unfortunately, it was not possible to incorporate an additional mathematical term for Phase 1 in the Khazaei model. Most likely, this is owing to the drastically different rate limiting sorption mechanism in this phase. The initial mass uptake is governed by convective liquid transfer into hygroscopic wood, which fills the open-ended lumina, whereas the behavior in Phases 2 and 3 suggests sorption that is limited by diffusive transfer within the cellular structure.

For this reason, Phase 1 was fitted as a separate term using a Fickian-like linear relationship of mass uptake as a function of the square root of time. However, it was found that the linear portion of the plot did not cross the origin, resulting in a ca. 3.5 *y* intercept (i.e., 3.5% mass uptake) for both *n*-hexadecane and water penetration in uncoated and epoxy-coated wood. The observed nonlinearity in the first part of the experimentally obtained sorption curve is believed to be a result of pronounced surface effects, e.g., the absorption of a monomolecular layer of liquid in open-ended pores. This process occurred when the liquid's uptake could not be measured accurately ($t < 7$ min) and thus was included as a constant, $M_{initial}$, in the empirical model developed ($M_{initial}$; Table 3; Fig. 2).

The opposite effect, i.e., a smaller slope near the origin, was observed by Siau (1995) for the diffusion of water into the wood. The decreased mass uptake was explained by evaporation from the surface and/or compressive stress at the surface until the initiation of relaxation of the cell-wall structure (Siau 1995). The differences in obtained results may be owing to the differences in the original water content of samples used in two sets of experiments. That is, the dryer the wood used, the slower the initial absorption of water, because of the slower formation of hydrogen bonds

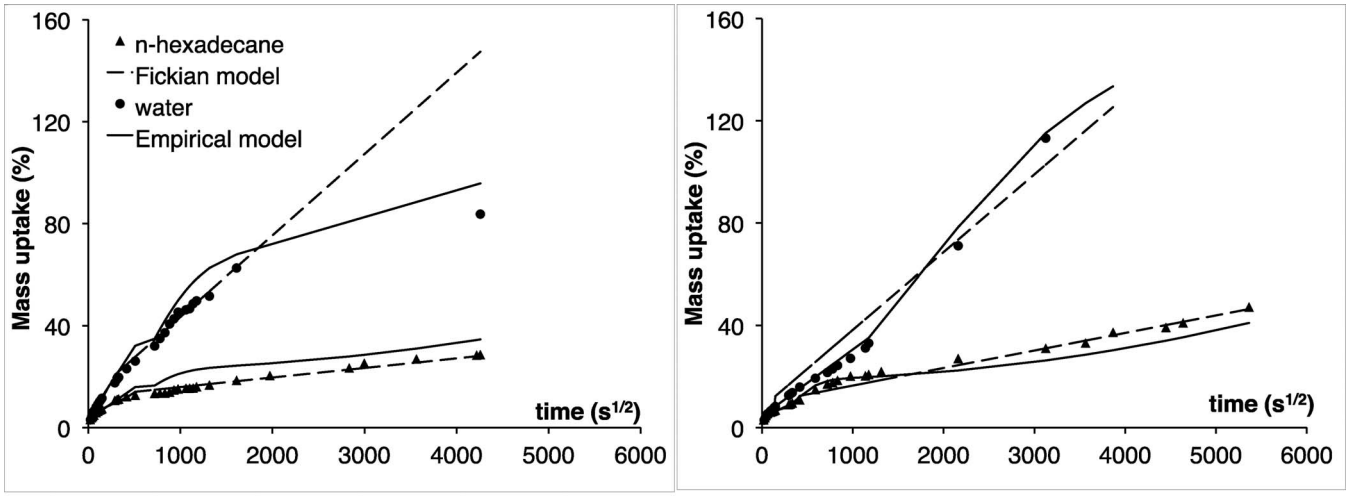

Figure 4.—A comparison between experimental data recorded for the one-dimensional sorption of n*-hexadecane or water through (a) uncoated wood and (b) epoxy-coated wood with theoretical data predicted by Fickian (Eq. 26) and empirical (Eq. 28) models.*

Table 3.—Estimated empirical model parameters and correlation of fit between theoretical and experimental data for the one-dimensional sorption of water and n*-hexadecane sorption through uncoated and epoxy-coated wood blocks.*[a]

Scenario	Penetrating liquid	Matrix	$M_{initial}$ (%)	k_1 (s^{-1})	t^* (h)	M^* (%)	M_{ret} (%)	k_2 ($\times 10^{-6}$ s^{-1})	k_3 ($\times 10^{-6}$ s^{-1})	R^2	RMSE
1	*n*-Hexadecane	Uncoated wood	3.2	0.03	72	15.8	22.6	2.4	0.66	0.92	2.9
2		Epoxy-coated wood	3.7	0.02	31	9.5	18.7	5.8	0.77	0.95	2.5
3	Water	Uncoated wood	3.8	0.06	72	32.1	65.1	1.4	1.7	0.95	5.4
4		Epoxy-coated wood	4.5	0.03	384	35.2	116.5	0.20	1.5	0.97	6.5

[a] All the parameters were determined by using Equation 28 as shown in Figure 2. $M_{initial}$, M^*, and M_{ret} are the mass uptake values at the start of Phases 1, 2, and 3, respectively; k_1, k_2, and k_3 are the sorption rate constants for Phases 1, 2, and 3, respectively; t^* is the time corresponding to M^*.

between this polar solvent and cellulose. Another potential factor may involve extractives on the wood surface that lower surface energies and can influence wetting.

The numerical values calculated using the empirical model for the times at which Phase 1 ended (i.e., t^*; Table 3) varied for different penetrating liquids and, surprisingly, were different from the supposedly similar times determined using the Fickian model (i.e., t_1 and t_2; Table 2). However, this variation may be because of the different interpretations of the transition time between Phases 1 and 2 in these models. The times t_1 and t_2 that were defined in the Fickian model as the endpoint times of the first and second sorption phases, correspondingly, actually represent the starting points of the next sorption processes while the previous process is still ongoing. Namely, t_1 represents the time when capillary rising starts to become significant, even though the simple absorption in surface open-ended tracheids is not yet completed, whereas t_2 represents the time when the liquid's transfer into wood via molecular diffusion becomes significant, although transport by capillary rising still contributes to the overall effective diffusion rate for some time.

By contrast, time t^* in the empirical model represents the completion of the absorption process, when capillary rising is the only significant sorption driving force (Table 3). In the case of *n*-hexadecane diffusion in epoxy-coated wood, the value of t^* was lower than that for uncoated wood, indicating a faster completion of the absorption process owing to sealing of the surface pores and, at the same time, the start of Phase 2 when absorption is dominated solely by capillary rising. Accordingly, lower mass uptake values at t^* (i.e., M^*; Table 3) in epoxy-coated samples were obtained. These results indicate that the observed fast initial absorption of nonpolar *n*-hexadecane proceeds only in open-ended and near-surface voids, whereas the bulk of the wood sample is filled at a slower rate and occurs by capillary rising and molecular diffusion.

The absorption process of polar water in either uncoated or epoxy-coated wood continued far beyond t_2 of Phase 2 (i.e., t_2, Table 2 vs. t^*, Table 3) and fully stopped at ca. $M^* = 30$ percent. The observed near-identical saturation parameter M^* (Table 3) values for water in coated and uncoated samples indicate that the absorption of water in wood proceeds not only through open-ended pores, as in the case of nonpolar *n*-hexadecane, but also through cell walls (Siau 1995). Yet, the kinetic parameters, both k_1 and particularly k_2, turned out to be smaller in the epoxy-coated wood samples than for uncoated wood because the epoxy-coated sides increased resistance to air displacement caused by water sorption (Table 3).

The goodness-of-fit statistics for the empirical model are presented in Table 3 as R^2 and RMSE. The comparison between experimental and predicted (by empirical model, Eq. 28) mass uptake data (Table 3) is shown in Figure 4. According to this information, the empirical model can reasonably predict the amount of *n*-hexadecane or water mass uptake at any specific time (even in long range). This model can also provide a valid description of the entire liquid mass uptake process, particularly during catastrophic floods, and to capture anomalous effects, which are often observed experimentally.

Effective surface area

The effective diffusion coefficient calculated in the Fickian model (D; Table 2) is a transport property of the sorption process. The empirical model, on the other hand, provides a kinetic parameter of the overall process, i.e., k_i as first-order sorption rate constants. The two models can be used together to calculate the effective surface areas of wood blocks subject to the sorption of either *n*-hexadecane or water (Table 4). Comparing these values to the actual physical experimental systems can provide insight that can help to explain the observed sorptive behavior. The actual physical surface area values from the wood block experiments were as follows: 1,482 mm^2 for the wood base, 3,020 mm^2 for the wood surface area in contact with the liquid (i.e., the wood base plus the area around the block with a height of 10 mm was used when estimating the effective diffusion coefficients listed in Table 2), and 2,310 mm^2 for the entire wood block.

Compared with these relatively large physical dimensions, the calculated effective surface areas for the Phase 1 sorption region turned out to be rather small, of a 10 mm^2 order of magnitude (Table 4). This value most likely reflects the physical size of lateral open-ended wood voids, filled during Phase 1 sorption, and suggests that the rest of the wood surface does not contribute to the initial liquid sorption into the wood.

As for Phase 2, the effective surface area calculated for *n*-hexadecane absorption matched the actual physical surface areas that are in contact with the penetrating liquid (including the area of the 10-mm in height wood block for uncoated wood samples). The observed pronounced difference between the effective surface areas for Phases 1 and 2 corroborates the proposed difference in the mechanism of nonswelling liquid penetration between these two phases.

In contrast to *n*-hexadecane, water can penetrate through the cell walls inside of the wood block, which leads to an increase in the effective contact surface areas compared with *n*-hexadecane. Supporting this assumption, the calculated effective surface area estimated from the models for Phase 2 was about two times greater than the actual physical surface area of the entire wood block in uncoated wood samples (Phase 2; Table 4). When the wood lateral pores

Table 4.—The calculated effective surface area for three sorption phases of the one-dimensional sorption of water or n*-hexadecane through uncoated and epoxy-coated wood blocks.*

Scenario	Penetrating liquid	Matrix	Effective surface area (mm^2)[a]		
			Phase 1 (A_{eff1})	Phase 2 (A_{eff2})	Phase 3 (A_{eff3})
1	*n*-Hexadecane	Uncoated wood	19	3,700	49
2		Epoxy-coated wood	37	2,100	63
3	Water	Uncoated wood	10	53,500	120
4		Epoxy-coated wood	22	414,000	130

[a] Effective surface areas were calculated using Equation 29, where D_i is the diffusion coefficient from Table 2, and k_i is sorption rate constant for that particular mass uptake phase from Table 3.

were sealed with epoxy, resistance to air displacement increased, and so the estimated effective surface area became even larger, more than 10 times higher than the physical surface area of the entire wood block.

In Phase 3, all the large-volume tracheids are filled, and sorption is postulated to be restricted to narrow capillaries. Thus, one would expect that a surface area calculation based on this region's sorption profile would be substantially lower than the actual physical cross-sectional area of the wood blocks used in the experiments. Consistent with this postulate, the calculated effective surface area is on the order of 10 to 100 mm^2 for *n*-hexadecane and 100 mm^2 for water (Phase 3; Table 4). Higher effective surface area values were calculated for the penetration of water, particularly in epoxy-coated wood samples, probably as a result of the enhanced penetration through cell walls, just as for Phase 2.

Conclusions

Comprehensive one-dimensional sorption profiles of *n*-hexadecane and water in uncoated and epoxy-coated wood samples generated from long-term (2-yr) experiments with wood blocks revealed three distinctly different sorption phases. Fickian and empirical models were developed that accurately match these profiles. These models were then used to calculate effective diffusion coefficients that represent the governing sorption mechanism (via the Fickian model) and the overall transport behavior (via the empirical model) of each phase. Both models can predict, with a reasonable accuracy, the *n*-hexadecane or water mass uptake at any specific time, within a long range of allotted times (e.g., months or even years) using the readily obtained data points just for the first few days. The calculated diffusion coefficients were then used to generate effective sorption surface areas that reflect how the liquid travels through wood's heterogeneous structure. Comparing these surface areas to the experimental physical cross-sectional areas of the wood blocks provides further corroboration that each of the three phases of sorption were governed by different factors and also reflected the differences in resistances to sorption for a nonpolar liquid, *n*-hexadecane, and a polar liquid, water.

Acknowledgments

Funding for this work was provided by the USDA Forest Products Laboratory (FPL) via cooperative agreements 04-JV-11111120-070 and 06-JV-11111120-073.

Literature Cited

Baronas, R., F. Ivanauskas, I. Juodeikiene, and A. Kajalavicius. 2001. Modelling of moisture movement in wood during outdoor storage. *Nonlinear Anal. Model. Control* 6(2):3–14.

Barrera-García, V. D., R. D. Gougeon, T. Karbowiak, A. Voilley, and D. Chassagne. 2008. Role of wood macromolecules on selective sorption of phenolic compounds by wood. *J. Agric. Food Chem*. 56(18):8498–8506.

Chin, J. W., T. Nguyen, and K. Aouadi. 1999. Sorption and diffusion of water, salt water, and concrete pore solution in composite matrices. *J. Appl. Polym. Sci*. 71(3):483–492.

Comstock, G. L. 1970. Directional permeability of softwoods. *Wood Fiber Sci*. 1(4):283–289.

Crank, J. 1975. The Mathematics of Diffusion. Clarendon Press, Oxford, UK. 414 pp.

Frihart, C. R. 2006. Wood adhesives vital for producing most wood products. *Forest Prod. J*. 61(1):5–12.

Kaiser, J.-A. 1999. Southern yellow pine: A long-time favorite. *Wood Prod*. 104(10):33–34.

Khazaei, J. 2008. Water absorption characteristics of three wood varieties. *Cercet. Agron. Moldova* XLI(2[134]):5–16.

Koponen, S. 1999. Effect of wood cell structure on diffusion properties—Sorption tests. *Helsinki Univ. Technol. LSEBP Publ*. 103:35–36.

Krabbenhoft, K. and L. Damkilde. 2004. A model for non-Fickian moisture transfer in wood. *Mater. Struct*. 37(273):615–622.

Kultikova, E. V. 1999. Structure and properties relationships of densified wood. M.S. thesis. Wood Science and Forest Products, Virginia Tech, Blacksburg.

Kumaran, M. K. 1999. Moisture diffusivity of building materials from water absorption measurements. *J. Therm. Envelope Build. Sci*. 22:349–355.

Malkov, S., V. Kuzmin, V. Baltakhinov, and P. Tikka. 2003. Modelling the process of water penetration into softwood chips. *J. Pulp Pap. Sci*. 29(4):137–143.

Malkov, S., P. Tikka, and J. Gullichsen. 2001. Towards complete impregnation of wood chips with aqueous solutions. Part 2: Studies on water penetration into wood chips. *Paper Timber* 83(6):468–473.

Marcovich, N. E., M. M. Reboredo, and M. I. Aranguren. 1999. Moisture diffusion in polyester-woodflour composites. *Polymer* 40(26):7313–7320.

Moghaddam, M. S., P. M. Claesson, M. E. P. Wålinder, and A. Swerin. 2013. Wettability and liquid sorption of wood investigated by Wilhelmy plate method. *Wood Sci. Technol*. 48(1):161–176.

Morgan, J. W. W. and D. F. Purslow. 1973. Physical and chemical aspects of preservative treatment by nonpressure methods. *Holzforschung* 27(5):153–159.

Petty, J. A. 1975. Relation between immersion time and absorption of petroleum distillate in a vacuum-pressure process. *Holzforschung* 29(4):113–118.

Petty, J. A. 1978a. Effects of solvent-exchange drying and filtration on the absorption of petroleum distillate by spruce wood. *Holzforschung* 32(2):52–55.

Petty, J. A. 1978b. Influence of viscosity and pressure on the radial absorption of non-swelling liquids by pine sapwood. *Holzforschung* 32(4):134–137.

Siau, J. F. 1995. Wood: Influence of Moisture on Physical Properties. Wood Science and Forest Products, Forest Virginia Tech, Blacksburg. 227 pp.

Smith, D. N. and D. F. Purslow. 1960. Preservative treatment of pine sapwood. *Timber Technol*. 68:67–71.

Stamm, A. J. 1946. Passage of liquids, vapors, and dissolved materials through softwoods. *USDA Tech. Bull*. 929:1–79.

Stamm, A. J. 1964. Wood and Cellulose Science. Ronald Press, New York.

Stone, J. E. and C. Forderrenther. 1956. Studies of penetration and diffusion into wood. *TAPPI* 39(10):679–683.

Tsuchikawa, S. and H. W. Siesler. 2003. Near-infrared spectroscopic monitoring of the diffusion process of deuterium-labeled molecules in wood. Part I: Softwood. *Appl. Spectrosc*. 57(6):667–674.